Structural and mechanistic mapping of a unique fumarate reductase

Paul Taylor[1], Sara L. Pealing[1,2], Graeme A. Reid[1], Stephen K. Chapman[2] and Malcolm D. Walkinshaw[1]

[1]Institute of Cell and Molecular Biology, University of Edinburgh, Mayfield Road, Edinburgh EH9 3JR, UK. [2]Department of Chemistry, University of Edinburgh, West Mains Road, Edinburgh EH9 3JJ, UK.

The 1.8 Å resolution crystal structure of the tetraheme flavocytochrome c_3, Fcc_3, provides the first mechanistic insight into respiratory fumarate reductases or succinate dehydrogenases. The multi-redox center, three-domain protein shows a 40 Å long 'molecular wire' allowing rapid conduction of electrons through a new type of cytochrome domain onto the active site flavin, driving the reduction of fumarate to succinate. In this structure a malate-like molecule is trapped in the enzyme active site. The interactions between this molecule and the enzyme suggest a clear mechanism for fumarate reduction in which the substrate is polarized and twisted, facilitating hydride transfer from the reduced flavin and subsequent proton transfer. The enzyme active site in the oxidized form is completely buried at the interface between the flavin-binding and the clamp domains. Movement of the cytochrome and clamp domains is postulated to allow release of the product.

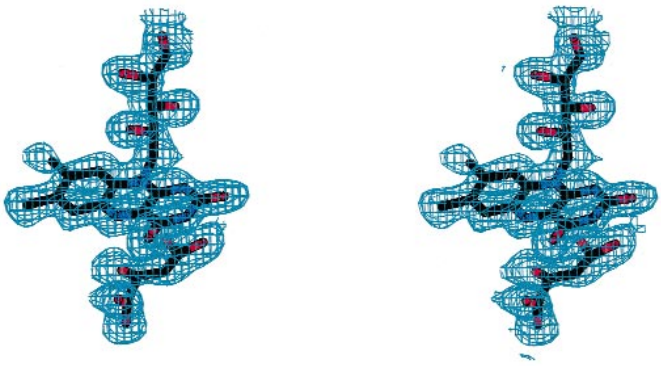

Fig. 1 $2F_o$ - F_c difference electron density. The stereo picture shows a portion of the final σ-weighted ($2F_o$-F_c) map about the flavin group and the modified substrate (BOBSCRIPT[29]).

The growth of *Shewanella frigidimarina* NCIMB400 under anaerobic conditions induces the synthesis of several novel cytochromes, the most abundant of which is a tetraheme Fcc_3 (M_r 63.8 kDa). The gene encoding Fcc_3 has been cloned and sequenced (Swissprot entry FRDA_SHEPU) and the protein product has been shown to be a unique respiratory fumarate reductase[1,2]. It differs from other bacterial fumarate reductases, which are multisubunit and anchored to the inner face of the cytoplasmic membrane[3]. In contrast Fcc_3 is a soluble, single chain enzyme found in the periplasm[4]. The N-terminal cytochrome domain contains four covalently bound heme groups and shows no significant sequence

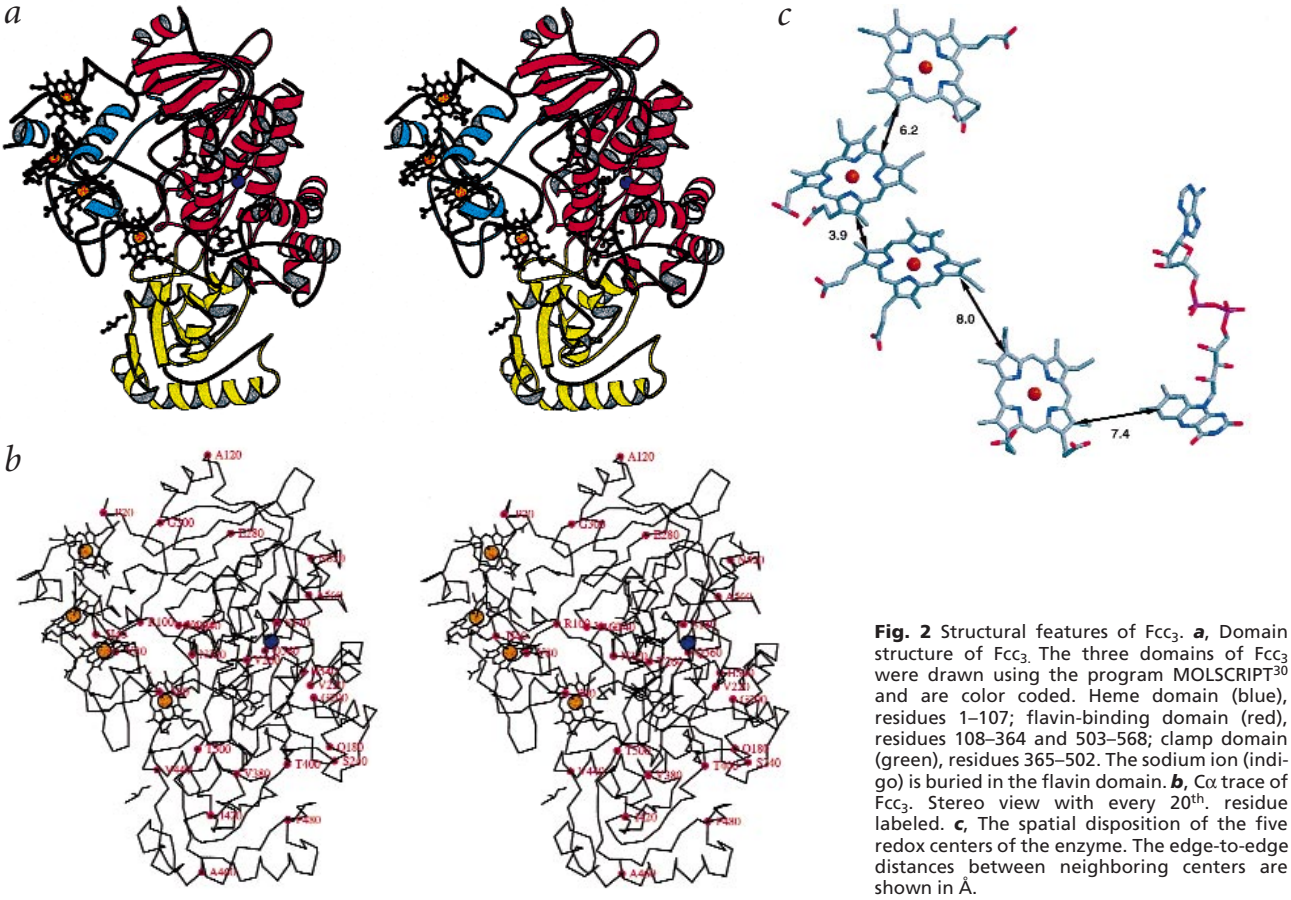

Fig. 2 Structural features of Fcc_3. ***a***, Domain structure of Fcc_3. The three domains of Fcc_3 were drawn using the program MOLSCRIPT[30] and are color coded. Heme domain (blue), residues 1–107; flavin-binding domain (red), residues 108–364 and 503–568; clamp domain (green), residues 365–502. The sodium ion (indigo) is buried in the flavin domain. ***b***, Cα trace of Fcc_3. Stereo view with every 20th. residue labeled. ***c***, The spatial disposition of the five redox centers of the enzyme. The edge-to-edge distances between neighboring centers are shown in Å.

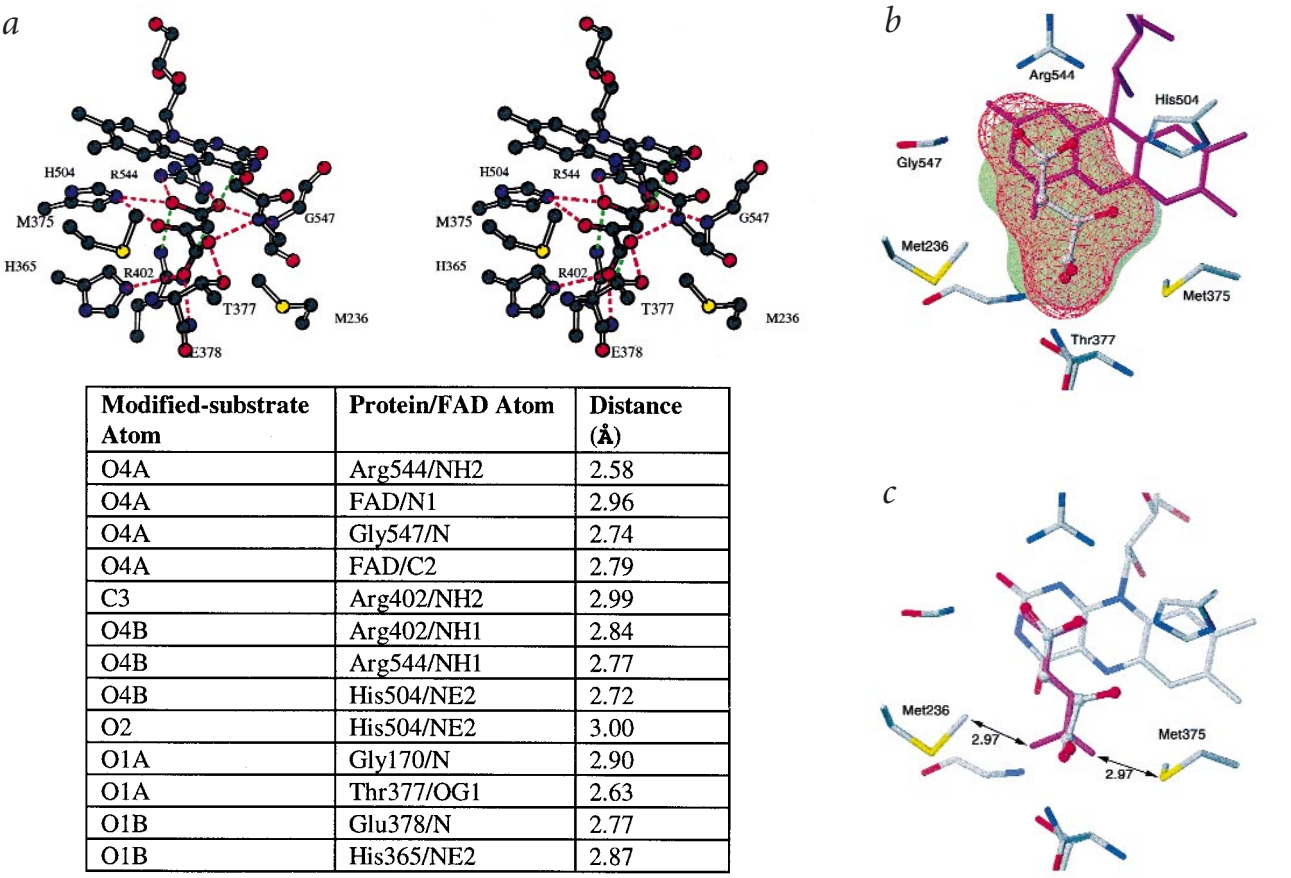

Modified-substrate Atom	Protein/FAD Atom	Distance (Å)
O4A	Arg544/NH2	2.58
O4A	FAD/N1	2.96
O4A	Gly547/N	2.74
O4A	FAD/C2	2.79
C3	Arg402/NH2	2.99
O4B	Arg402/NH1	2.84
O4B	Arg544/NH1	2.77
O4B	His504/NE2	2.72
O2	His504/NE2	3.00
O1A	Gly170/N	2.90
O1A	Thr377/OG1	2.63
O1B	Glu378/N	2.77
O1B	His365/NE2	2.87

Fig. 3 The active site of Fcc_3. ***a***, Stereo MOLSCRIPT[30] representation of the environment of the modified substrate. Hydrogen bonds are shown as red dashed lines. Other short contacts are shown as green dashed lines. Distances are also tabulated showing hydrogen bonds and short nonbonded contacts (<3.1 Å) involving the modified substrate. ***b***, Connolly surfaces of the available active site volume (green) and substrate-occupied volume (red). The Connolly surface of the available volume in the substrate binding site (transparent green surface) is almost completely filled by the substrate intermediate molecule. The Connolly surface of the substrate intermediate molecule shown as a wire representation colored red. ***c***, An overlay of a modeled planar fumarate (magenta) and the modified substrate. Short contacts between the modeled fumarate molecule and the two clamping methionine residues are shown. The resulting twist in the conformation of the carboxyl group is important in the enzyme mechanism.

similarity to any cytochrome of known three-dimensional structure. The flavin adenine dinucleotide (FAD) binding domain is related by sequence to the flavoprotein subunits of the membrane-bound fumarate reductases and succinate dehydrogenases[1]. The recent X-ray structure of the *E. coli* fumarate reductase respiratory complex[5] provides insight into the general architecture of an iron-sulfur based reductase, but at 3.3 Å shows little detail at the active site. In contrast the high resolution structure of Fcc_3, a cytochrome-linked reductase, provides the first insight into the detailed mechanism of fumarate reduction. These new fumarate reductase structures together with the X-ray structures of cytochrome *c* oxidase[6] and the cytochrome bc_1 complex[7], greatly enhance our molecular understanding of respiratory mechanisms.

Overview of the structure

The initial electron density map with phases from the anomalous iron signal was of exceptionally high quality and most of the chain could be unambiguously traced from the initial 2.4 Å map. The four heme groups and the FAD group were easily identified. Data to 1.8 Å were used to refine the structure to a final R-factor of 19.2% (Table 1) and the quality of the final electron density map is shown in Fig. 1.

The single polypeptide chain of 571 amino acids folds into three distinct domains (Fig. 2*a*,*b*). The N-terminal, 100 amino acid cytochrome domain containing four heme groups is tethered to the flavin domain by a charged bent helix linker (residues 100–110). The flavin domain (residues 111–364 and 503–571 colored red in Fig. 3) holds the noncovalently bound FAD group. The overall fold of the FAD binding domain has a structural and topological similarity to known FAD binding proteins, although the sequence similarity is poor: there is 18% sequence identity with lipoamide dehydrogenase[8] and 19% identity with glutathione reductase[9]. An even weaker sequence similarity is found with NADH peroxidase[10] despite the fact that superposition of the structures indicates that ~90 amino acids show a reasonable structural correspondence. The most closely related proteins of known structure are L-aspartate oxidase[11] and *E. coli* fumarate reductase[5], which have sequence identities of 38% and 45%, respectively, over the length of the 121 residues corresponding to the Rossmann fold. A fit of the flavin domain of Fcc_3 onto the flavin binding domain of L-aspartate oxidase gives a residual mean standard deviation (r.m.s.d.) of 1.7 Å for 103 corresponding Cα atoms. Buried within the flavin domain is an octahedrally coordinated sodium ion (Fig. 2*a*,*b*) that is close to the active site and may well play a structural or regulatory role[12].

The clamp domain of Fcc_3 (residues 365–502, shown in yellow in Fig. 2*a*) is likely to be involved in controlling access of substrate to the active site. It consists of seven short helical

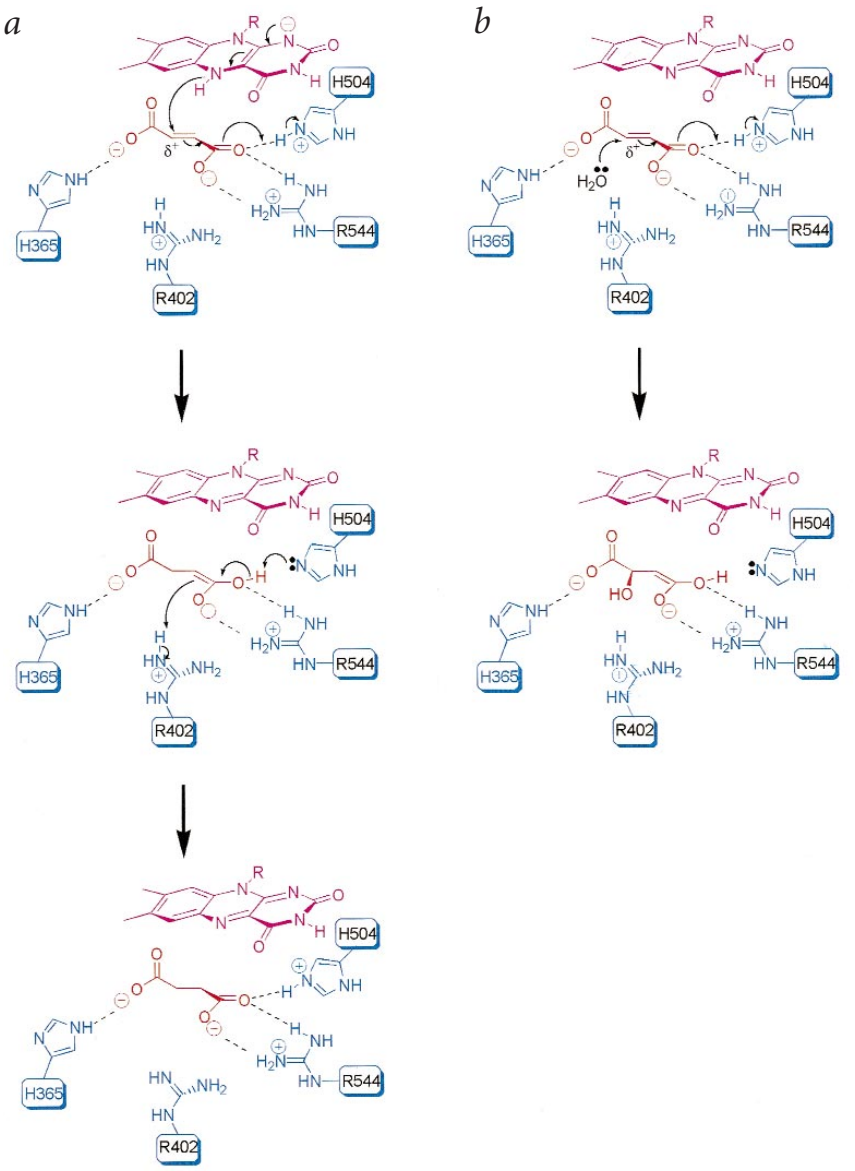

Fig. 4 Reaction mechanisms at the Fcc_3 active site. ***a***, Schematic representation of the mechanism of fumarate reduction by Fcc_3. Catalysis is initiated by the binding of fumarate at the active site. The C1 carboxylate group of fumarate (to the left in this representation) is twisted out of plane by the closure of the clamp domain and the resulting steric constraints imposed by the side chains of Met 236 and Met 375 (Fig. 3*d*) and by hydrogen bonding to His 365. The substrate C4 carboxylate is bound in a very positively charged environment involving interactions with His 504, Arg 544 and Arg 402. The combination of these effects results in polarization of the C2–C3 bond with the build up of positive charge at C2, facilitating hydride transfer from N5 of the reduced flavin to the *si*-face of the substrate. Arg 402 which is only 2.99 Å from C3, is ideally positioned for proton transfer, resulting in the formation of the product, succinate. ***b***, Proposed mechanism for the formation of the hydrated intermediate at the active site of the oxidized enzyme. In the oxidized flavocytochrome c_3, as is the case in the crystal, there is no hydride available to attack the substrate C2 atom. Instead, water acts as a nucleophile attacking the *re*-face. The resulting intermediate, which is shown in the electron density to have R-stereochemistry at C2, is trapped at the active site in the crystal. ***c***, Conservation of active site residues in fumarate reductases and succinate dehydrogenases. Segments of the sequence of Fcc_3 are aligned with the corresponding regions of the flavoprotein subunits of the fumarate reductases from *E. coli* (frda_ecoli) and *Wolinella succinogenes* (frda_wolsu) and the succinate dehydrogenases from *E.coli* (dhsa_ecoli) and *Saccharomyces cerevisiae* (dhsa_yeast) to highlight the conservation around active site residues. The following residues are highlighted in red: His 365 and Thr 377 (top left), Arg 402 (top right), His 504 (bottom left) and Arg 544 (bottom right).

stretches wrapped round a four-stranded antiparallel sheet. There is no obviously similar three-dimensional structure and searches using the programs VAST[13], TOPS[14] and DALI[15] provide only weakly similar folds.

Relationship of the five redox cofactors

The redox properties of Fcc_3 have recently been investigated using protein film voltammetry, allowing the reduction potentials of all five redox cofactors to be determined[16]. The 'dog leg' arrangement of the four heme groups is unique in the family of cytochromes c_3. The edge-to-edge distances between the heme groups vary from 3.9 Å to 8.0 Å (Fig. 2*c*) that are ideal for efficient inter-heme electron transfer. Heme 4 is 7.4 Å (edge-to-edge) from the FAD. This compares well to the heme–flavin distance of 9.7 Å seen in flavocytochrome b_2 (ref. 17), one of the few other structurally characterized flavocytochromes. The overall positioning of the redox centers in Fcc_3 represents a 40 Å long 'molecular wire' running through the protein which enhances our understanding of previously published kinetic and thermodynamic data[16,18].

The reduction potential for the FAD is -152 mV and the four hemes have values of -238 mV, -196 mV, -146 mV, -102 mV[16]. In common with other *c*-type cytochromes, the hemes are covalently linked to two cysteines in the CxxCH motif. In all cases histidines provide the fifth and sixth ligands for the iron. The structure confirms that, as predicted by electron paramagnetic resonance (EPR) spectroscopy[19], two hemes have their

Table 1 Data collection, phasing and refinement statistics

MAD data reduction statistics (24.0–2.4 Å)					
Data set	Wavelength (Å)	Unique reflections	Completeness (%)	<I>/<σ(I)>	R_{merge}(%)[1]
Anom. Peak	1.736	25,101	98.7	20.9	7.7
Infl. Point	1.738	20,031	79.1	22.1	8.8
Remote	1.488	22,628	89.8	18.6	6.2
Phasing (24.0–2.4 Å)					
Overall Figure of merit	SOLVE: 0.47	DM: 0.66			
Refinement (24.0–1.8 Å)					
Unique reflections			Completeness (%)	<I>/<σ(I)>	R_{merge}(%)[1]
54,988			92.5	13.2	8.3
R_{cryst} (%)[2]			19.2		
R_{free} (%)[2]			26.7		
R.m.s.d. from restraint values					
Bond length (Å)		0.007			
Bond angle distances (Å)		0.022			
Ramachandran analysis					
Most favored		87.1%			
Additionally allowed		12.5%			
Generously allowed		0.4%			

[1] $R_{merge} = \Sigma|<I> - I| / \Sigma<I>$; over all reflections.
[2] $R_{cryst} = \Sigma|F_o - F_c| / F_o$; R_{free} calculated with 10% data withheld from refinement.

imidazole ligating groups parallel and two perpendicular to each other, and these are possibly involved in fine tuning the reduction potentials of the hemes. There is no significant sequence conservation between this tetraheme domain and any other heme-containing proteins the X-ray structures of which are known. There is, however, an interesting similarity in the arrangement of three of the heme groups in hydroxylamine oxidoreductase[20].

Mechanism of fumarate reduction

The crystallization medium contained a 10 mM solution of fumarate, well above the K_M of 25 μM[19], suggesting that the active site of Fcc_3 should be fully occupied. However, the difference electron density map clearly shows the presence of a hydrated malate-like molecule in the enzyme active site of Fcc_3. It is unlikely that this molecule is oxaloacetate because the protein is crystallized from the fully active enzyme that was purified in the complete absence of oxaloacetate. The malate-like molecule is held tightly by 11 hydrogen bonds (Fig. 3*a*) and sits in a close-fitting binding site that is completely inaccessible to solvent (Fig. 3*b*). The tight steric constraints of the active site require that the C1 carboxyl group twists out of the plane. A model of an idealized planar fumarate was fitted onto the observed malate-like molecule by superposing the C4 carboxyl groups (Fig. 3*c*). The modeled fumarate shows short contacts between the C1 carboxyl group and the side chains of Met 236 and Met 375. This interaction provides the drive to twist the substrate out of the planar conformation, which has the additional effect of weakening the conjugation throughout the molecule. The exceptionally polar hydrogen bonding environment of the C4 carboxyl group, with contributions from two arginines and a histidine, acts to polarize the fumarate. The combined steric and electronic effects then reinforce each other to generate considerable positive charge at C2 (Fig. 4), making it amenable to the subsequent nucleophilic attack. In the biologically relevant mechanism (Fig. 4*a*), a hydride on N5 of the flavin ring would be positioned less than 3.2 Å from C2, poised to attack the *si*-face of the C2 center. Under the oxidizing conditions used for crystal growth, hydride attack is not possible and instead there is attack by H_2O on the *re*-face to provide the observed product, which has R-stereochemistry at C2 (Fig. 4*b*).

In the final rounds of refinement, bond distance and bond angle restraints (consistent with malate) for the substrate were removed and the model converged on a geometry consistent with the product shown in Fig. 4*b*. In particular, the C4-C3-C2 angle refined to 120° while that of C1-C2-C3 refined to 110°. The interaction between Arg 402 NH2 and substrate C3 which are separated by 2.99 Å is then understood in terms of the interaction between the δ^+ charge of the arginine side chain with the delocalized π-electrons of the C3–C4 partial double bond. The geometry of the ligand and the close NH–C3 contact show that the substrate has been hydroxylated but not yet protonated (by the arginine) and we have trapped a stable intermediate in the active site of the crystal. Furthermore, the intermediate defined in the Fcc_3 structure specifies the time course of the reaction, showing that hydride transfer to C2 occurs before proton transfer to C3.

The enclosed nature of the active site (Fig. 3*b*) suggests that a conformational change is required to allow succinate product to diffuse out and fumarate substrate to enter. An insight to this mechanism comes from the X-ray structure of the two domain L-aspartate oxidase[11] which has been solved in an open (FAD-free) conformation. The clamp domain of L-aspartate oxidase shows 30% sequence identity to the clamp domain of Fcc_3. The displacement of the cytochrome and clamp domains of Fcc_3 with respect to the flavin domain would allow free access to the substrate binding pocket and could be achieved by conformational changes in the interdomain linking peptides 364–366 and 500–503, and the long tether (residues 100–108).

One important consequence of this X-ray crystal structure is its relevance to other members of the fumarate reductase/succinate dehydrogenase family, which are key components of respiratory pathways. There are four key aspects to the Fcc_3 mechanism: (i) delivery of electrons to the flavin, (ii) the highly polarized recognition site (iii) the induced twist in the fumarate substrate and (iv) the domain movement to allow release of the

substrate. The extensive sequence similarity between the flavin-binding region of Fcc_3 and other fumarate reductases/succinate dehydrogenases is consistent with the idea that a common catalytic mechanism operates for all members of this important enzyme group. The key residues involved in substrate binding and catalysis (Arg 402, Arg 544, His 504, His 365, Thr 377) are conserved in all members of this enzyme family (Fig. 4*c*). The membrane-bound fumarate reductases and succinate dehydrogenases, however, use iron-sulfur clusters as electron mediating groups[3]. Thus, the X-ray structure of Fcc_3 provides a major insight into a general mechanism for fumarate reduction and identifies a unique pathway for electron flow to the flavin, mediated by the four heme groups.

Methods

Structure determination. Protein purification and preliminary crystallographic work has been published[21]. Native data were collected on a MarResearch image plate at station 7.2 at the SRS in Daresbury, with MAD data collected using a similar instrument at the EMBL outstation DESY in Hamburg. For all data sets the processing was carried out using the HKL package[22]. All four iron atoms were located using anomalous and difference Patterson maps calculated with the CCP4 suite[23]. Subsequently the program SOLVE[24] was used and the same iron positions were determined. When phase estimates from SOLVE were solvent-flattened using the program DM[25], the heme groups and attached amino acids were visible in the electron density as was the FAD. In a map calculated using 2.4 Å data it was possible to trace ~80% of the polypeptide chain using the graphics program WITNOTP[26]. This model was then refined using the maximum likelihood torsional dynamics algorithm from CNS[27]. Refinement was completed using the 1.8 Å native data set with the program SHELXL-97 (ref. 28), using the same test set of reflections as had been used with CNS. Restraints for the heme groups were calculated from the CNS parameter file and for the FAD from two small molecule crystal structures (Cambridge Crystallographic Database codes HMADPH and VEFHUJ10). The model consists of residues 1–568, four hemes, the FAD, a modified substrate molecule, one sodium ion, a glycerol molecule and 584 water molecules. One *cis* peptide bond, between Ala 175 and Trp 176, was clearly identified. The three C-terminal residues of the (569–571) were not located.

Coordinates. The atomic coordinates have been deposited in the Protein Data Bank (accession code 1qjd).

Acknowledgments

We thank A. Mattevi for the L-aspartate oxidase coordinates, R. Baxter, S. Flitsch, D. Gerloff and S. Webster for helpful discussion and D. Alexeev and A. Gonzalez for help in X-ray data collection. We thank the BBSRC and EMBL for access to synchrotron radiation sources at Daresbury and Hamburg. This work was funded by the UK Biotechnology and Biological Sciences Research Council.

Correspondence should be addressed to M.D.W. *email: m.walkinshaw@ed.ac.uk*

Received 6 August, 1999; accepted 30 September, 1999.

1. Pealing, S.L., Black, A.C., Manson, F.D.C., Ward, F.B., Chapman, S.K. & Reid, G.A. *Biochemistry* **32**, 3829–3829 (1993).
2. Gordon, E.H.J., Pealing, S.L., Chapman, S.K., Ward, F.B. & Reid, G.A. *Microbiology-UK* **144**, 937–945 (1998).
3. Ackrell, B.A.C., Johnson, M.K., Gunsalus, R.P. & Cecchini, G. in *Chemistry and Biochemistry of Flavoenzymes* (ed Muller, F.) 229–297 (CRC Press, Boca Raton, Florida; 1992).
4. Reid, G.A., *et al. Biochem. Soc. Trans.* **26**, 418–421 (1998).
5. Iverson, T.M., Luna-Chavez, C., Cecchini, G. & Rees, D.C. *Science* **284**, 1961–1966 (1999).
6. Iwata, S., Ostermeier, C., Ludwig, B. & Michel, H. *Nature* **376**, 660–669 (1995).
7. Zhang, Z.L., *et al*. *Nature* **392**, 677–684 (1998).
8. Mattevi, A., Obmolova, G., Kalk, K.H., van Berkel, W.J.H. & Hol, W.G.J. *J. Mol. Biol.* **230**, 1200–1215 (1993).
9. Mittl, P.R.E. & Schulz, G.E. *Protein Sci.* **3**, 799–809 (1994).
10. Yeh, J.I., Claiborne, A. & Hol, W.G.J. *Biochemistry* **35**, 9951–9957 (1996).
11. Mattevi, A. *et al. Structure* **7**, 1–9 (1999).
12. Woehl, E. & Dunn, M.F. *Biochemistry* **38**, 7118–7130 (1999).
13. Madej, T., Gibrat, J.F. & Bryant, S.H. *Proteins Struct. Func. Genet.* **23**, 356–369 (1995).
14. Flores, T.P., Moss, D.S. & Thornton, J.M. *Protein Engineering* **7**, 31–37 (1994).
15. Holm, L. & Sander, C. *J. Mol. Biol.* **233**, 123–138 (1993).
16. Turner, K.L., Doherty, M.K., Heering, H.A., Armstrong, F.A., Reid, G.A. & Chapman, S.K. *Biochemistry* **38**, 3302–3309 (1999).
17. Xia, Z.X. & Mathews, F.S. *J. Mol. Biol.* **212**, 837–863 (1990).
18. Schroder, I., Gunsalus, R.P., Ackrell, B.A.C., Cochran, B. & Cecchini, G. *J. Biol. Chem.* **266**, 13572–13579 (1991).
19. Pealing, S.L., Cheesman, M.R., Reid, G.A., Thomson, A.J., Ward, F.B. & Chapman, S.K. *Biochemistry* **34**, 6153–6158 (1995).
20. Igarashi, N. *et al*. *Nature Struct. Biol.* **4**, 276–284 (1997).
21. Pealing, S.L. *et al. J. Struct. Biol.* **127**, 76–78 (1999).
22. Otwinowski, Z. & Minor, W. *Methods Enzymol.* **276**, 307–326 (1997).
23. Collaborative Computational Project Number 4, *Acta.Crystallogr. D* 50, 760–763 (1994).
24. Terwilliger, T.C. & Berendzen, J. *Acta Cryst. D* **55**, 849–861 (1999).
25. Cowtan, K. *Joint CCP4 and ESF-EACBM Newsletter on Protein Crystallography* **31**, 34–38 (1994).
26. Widmer, A. *WITNOTP* (Novartis A.G., Basel, Switzerland; 1999).
27. Brunger, A.T., *et al*. *Acta Crystallogr.* D **54**, 905–921 (1999).
28. Sheldrick, G.M. *SHELX-97* (University of Goettingen, Germany, 1997).
29. Esnouf, R.M. *J. Mol. Graphics* **15**, 132–136 (1997).
30. Kraulis, P.J. *J. Appl. Crystallogr.* **24**, 946–950 (1991).